IEEE Access
Multidisciplinary ⋮ Rapid Review ⋮ Open Access Journal

Received 2 September 2022, accepted 18 September 2022, date of publication 28 September 2022,
date of current version 21 October 2022.

Digital Object Identifier 10.1109/ACCESS.2022.3210566

RESEARCH ARTICLE

Nonlinear Time-Delay Observer-Based Control to Estimate Vehicle States: Lateral Vehicle Model

HICHAM EL AISS[1], (Member, IEEE), KARINA A. BARBOSA[1], (Senior Member, IEEE), AND ANDRÉS A. PETERS[2], (Member, IEEE)
[1]Department of Electrical Engineering, Universidad de Santiago de Chile, Santiago 9170022, Chile
[2]Faculty of Engineering and Sciences, Universidad Adolfo Ibáñez, Santiago 7941169, Chile

Corresponding author: Hicham El Aiss (hicham.elais@usach.cl)

This work was supported by the Facultad de Ingenieria Universidad, Santiago de Chile. The work of Hicham El Aiss was supported by the Fondo Nacional de Desarrollo Científico y Tecnologico-Fondecyt, Chile, under Grant 3190378. The work of Karina A. Barbosa was supported by the Universidad de Santiago de Chile, Dirección de Investigación Científica y Tecnológica (DICYT), under Grant 062113AB. The work of Andrés A. Peters was supported by the Agencia Nacional de Investigación y Desarrollo (ANID) Fondo Nacional de Desarrollo Científico y Tecnológico (FONDECYT) under Grant 11221365.

ABSTRACT This paper deals with the state estimation and control problem for nonlinear lateral vehicle dynamics with time delays. First, a novel time-varying delay vehicle model described as a Takagi-Sugeno fuzzy model is presented. In particular, it is considered that the lateral force contains an air resistance term which is assumed to be a quadratic function of the lateral vehicle velocity. A time-varying delay has been included in the vehicle states by a simple formula in order to capture brake actuation aspects or other practical aspects that may generate a delayed response, while the nonlinear part of the vehicle model is described as a Lipschitz function. A Takagi-Sugeno time-delay observer-based control that satisfies the Lipschitz condition is proposed to get closed-loop stability conditions. These results generalize existing ones in the literature on lateral dynamics control. Additionally, we provide a new methodology for the controller and observer gains design that can be cast as linear matrix inequality constraints. Finally, we illustrate our results with numerical examples, which also reveal the negative effect of not considering the presence of delays in the controller design.

INDEX TERMS Lateral vehicle model, time-varying delay, observer-based control, T-S fuzzy model, LMIs.

I. INTRODUCTION

Every year around the world, over a million people are killed and millions are injured in car accidents. This can be seen as a huge road war in some countries, since many people risk their lives every day. Researchers have tried to tackle the challenge of road traffic safety from different angles (see for example [1] and the references therein). The study and development of vehicular systems play a significant role in overcoming this challenge, and the automotive engineering industry and research laboratories in this field have constantly been striving to make vehicles comfortable, efficient and safe. In this regard, this work delves in the topic of observer-based control systems for lateral vehicle dynamics, and in particular, expanding the analysis to consider time-varying delays with nonlinear vehicle dynamics.

The associate editor coordinating the review of this manuscript and approving it for publication was Wonhee Kim.

The research on lateral vehicle dynamics and their control design has received a great deal of attention in the recent decade [2], [3], [4], [5]. Model predictive control (MPC) schemes have been used to track a lateral vehicle desired path [6], [7], [8]. In [9], a state-feedback control is investigated for the lateral motion of an intelligent vehicle. A great deal of work has been done to estimate and control lateral vehicle systems. The active yaw stabilizer (AYS) system was proposed in [2] to improve vehicle lateral stability control. In [3], the authors used the steer-by-wire (SBW) system to improve vehicle safety, maneuverability and steering flexibility. In [4], the authors investigated a two-dimensional state portrait analysis to enable the control designer to test the stability and trajectories of the vehicle system. In addition, many approaches and methodologies addressing vehicle systems' problems are discussed in [4] and the references therein. In [10], the authors used a fuzzy control method for vehicle systems to increase stability and reduce the rollover risk when

considering the lateral forces' nonlinearity using the Takagi-Sugeno (T-S) representation.

It is well known that many physical, industrial and engineering systems are nonlinear. In this context, the T-S fuzzy approach has become essential for dealing with complex nonlinear systems, since fuzzy models can adequately describe several natural systems. These systems are competent to describe a large class of nonlinear systems using fuzzy IF-THEN rules, which are described in the form of local linear or affine models connected by fuzzy membership functions [10], [11]. Recently, fuzzy observer-based control has attracted the attention of several researchers due to the importance of unmeasured internal states of real systems. Several studies have dealt with fuzzy observer design problems for continuous systems [10], [11], [12]. In [10], the authors used a fuzzy observer-based control to evaluate the vehicle states, while in [11], the observer-based control strategy was used to control T-S fuzzy descriptor systems with time-varying delays and a H_∞ performance index.

Researchers have also studied the delay-free lateral vehicle dynamics, and several mathematical models have been suggested [13], [14], [15]. However, most of these models are derived by using assumptions and approximations, which can turn into the loss of critical information, especially when dealing with safety related behaviors of nonlinear models. In particular, the delay information could be regarded as an essential component of an accurate model for lateral vehicle dynamics, when considering the effect that irregular or asymmetrical road conditions could have on the steering. This work introduces a time-varying delay function that aims to recover information that would be otherwise lost when applying approximations to deal with delays in the real model. We believe that this can help to get a new time-delay model that may perform better for observer-based control applications.

Time delays have not attracted much interest from researchers in the field of lateral vehicular motion. However, it is well known that delay occurs in most natural systems and is part of many processes. For example, delays may occur as a result of the transmission of information between various parts of a system and because of limited information processing capabilities [11], [16], [17]. Furthermore, delays can not be ignored, as they can cause instability and system performance degradation [18], [19], [20]. Several works have been reported that deal with a time-varying delay system, see for comparison purposes [11], [16], [17] and the references therein.

The first contribution of the present work is to propose a novel lateral vehicle model by introducing a time-varying delay in its states. The proposed model is more general than those in the literature [10], [21], which can be recovered as the time-varying delay tends to zero. Also, the lateral forces have been represented by the Takagi-Sugeno (T-S) model, which globalizes the lateral forces given in other works such as [10], [21], and [11]. The nonlinear part not introduced in the T-S model is considered to be a Lipschitz function. The second contribution is the proposal of a T-S observer-based control to estimate the yaw rate and side-slip angles, together with a new methodology for simultaneously designing the observer and controller gains based on LMI conditions.

The outline of this paper is as follows: Section II presents the notation and nomenclature used throughout the paper. In Section III, we present the lateral vehicle model under study. In contrast, Section IV presents the problem formulation and the main contributions of this work regarding observer-based control design. Section V presents simulation results and their analysis, illustrating the theoretical results and the design methodology for the proposed observer-based control scheme. Finally, conclusions and future work are placed in VII.

II. NOTATION AND NOMENCLATURE

We use $\mathbb{R}^n$ to denote the n-dimensional Euclidean space, and $\mathbb{R}^{n\times n}$ to denote the set of all $n \times n$ real matrices. For a matrix $X \in \mathbb{R}^{n\times n}$, X^{-1} and X^T will denote the inverse and the transpose of X, respectively. Asterisks $(*)$ will denote the symmetric part of a symmetric matrix. The notation $X > 0$ means that the matrix X is real symmetric positive definite. We denote by I (I_n) the identity matrix of adequate order (n) and by $\mathbf{0_{n\times m}}$ the $n \times m$ null matrix. We define $sym(A) = A + A^T$. Finally, $diag\{\dots\}$ denotes a block-diagonal matrix.

NOMENCLATURE

(See Fig. 1):

F_x	Is a longitudinal force.
F_y	Is a lateral force.
M_z	Is the yaw moment, pointing in the positive z direction.
$V_x(t)$	Is the longitudinal velocity.
$V_y(t)$	Is the lateral velocity.
$\dot{\psi}$	Is the yaw rate.
I_z	Is yaw moment of inertia.
F_{yf}	Is the front tire force.
F_{xr}	Is the rear tire force.
a_1	Is the distance from the center of gravity to the front tires.
a_2	Is the distance from the center of gravity to the rear tires.
$\delta(t)$	Is the front wheel steering angle.
$\alpha_f(t)$	Is the front tire side-slip angle between wheel x-axis and the velocity v.
$\alpha_r(t)$	Is the rear tire side-slip angle between wheel x-axis and the velocity v.
C_f	Is the cornering stiffness of the front tires.
C_r	Is the cornering stiffness of the rear tires.
$\beta_f(t)$	Is the front side-slip angle of wheel vehicle.
$\beta_r(t)$	Is the rear side-slip angle of wheel vehicle.
$\beta(t)$	Is the vehicle side-slip angle.

III. VEHICLE MODEL

This section describes the vehicular model to be studied.

A. INITIAL VEHICLE MODEL

The bicycle model (Fig. 1) describes the essential nonlinear lateral dynamics of the vehicle. They balance complexity and computation efficiency. The first contribution of this work is to propose a new vehicle model that describes the relationship between the relevant variables of the lateral dynamics, for example, the yaw rate and the side-slip angle (see Fig. 1).

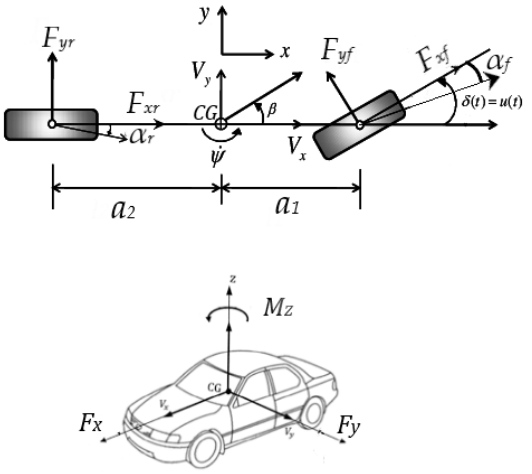

FIGURE 1. Vehicle model.

The bicycle vehicle model (single-track model) was invented in 1940 and is still widely used today [22], [23], [24]. Several significant omissions and simplifications are included in the bicycle model, which effectively reduces the degree of freedom of the model without affecting the vehicle's dynamic behavior in the linear range. The bicycle model can be converted to a computer simulation model and can be used to quickly and easily analyze vehicle behavior [25], [26]. Based on the assumptions and simplifications considered in [25], [26], the geometric relationships for the bicycle model can be developed as shown in Fig. 1.

By using Newton-Euler motion equations for a rigid vehicle in the body coordinate frame connected to the vehicle at its mass center, the following equations are obtained [27]:

$$\begin{aligned} F_x &= m\dot{V}_x(t) - m\dot{\psi}(t)V_y(t), \\ F_y &= m\dot{V}_y(t) + m\dot{\psi}(t)V_x(t), \\ M_z &= \ddot{\psi}(t)I_z, \end{aligned} \tag{1}$$

where m is the mass of the vehicle, and M_z is the yaw moment, pointing in the positive z direction. We can now consider the four-wheel vehicle whose longitudinal and lateral forces are projected on the body coordinate as follows

$$\begin{aligned} F_x &= 2F_{xf}\cos\delta(t) - 2F_{yf}\sin\delta(t) + 2F_{xr}, \\ F_y &= 2F_{xf}\sin\delta(t) + 2F_{yf}\cos\delta(t) + 2F_{yr}, \\ M_z &= 2a_1F_{yf}\cos\delta(t) + 2a_2F_{xf}\sin\delta(t) - 2a_2F_{yr}. \end{aligned} \tag{2}$$

The nonlinear model given in (2) has been obtained by assuming that the left and right wheels have the same longitudinal and lateral force. Moreover, in [27], [28], and [21], the authors considered the steer-angle $\delta(t)$ to be small, to obtain linear models for the yaw moment, and the longitudinal and lateral forces. Based on this approximation, large amount of work has been done, in order to deal with the challenges arising from nonlinear terms in the lateral vehicle dynamics.

Considering small steer-angle $\delta(t)$ approximations, the above nonlinear forces in (2) can be simplified as (see for instance [27], [28] and [21]):

$$\begin{aligned} F_x &= 2F_{xf} + 2F_{xr}, \\ F_y &= 2F_{yf} + 2F_{yr}, \\ M_z &= 2a_1F_{yf} - 2a_2F_{yr}. \end{aligned} \tag{3}$$

In [21] and [10], the authors have considered that the lateral forces depend on the front and rear side-slip angles $\alpha_f(t)$ and $\alpha_r(t)$, and the relationship between these forces and the angles $\alpha_f(t)$ and $\alpha_r(t)$ to be linear. By assuming such approximations, these relationships can be expressed as

$$F_{yf} = -C_{\alpha f}\alpha_f(t), \quad F_{yr} = -C_{\alpha r}\alpha_r(t). \tag{4}$$

Notice that the relationships given in (4) are valid for bounded side-slip angles, which implies that they are applicable when the vehicle velocity is small. Thus, the conditions in (4) are valid in the linear region (steady-state), which makes dynamic relationships much more complex. Furthermore, we can see that the lateral forces suggested in (4) tend to be constant for all vehicle wheels. This is not generally true since the lateral force generated by each wheel is different from the ones produced by the other wheels. In this context, we consider the nonlinearities of the lateral forces by using the Takagi–Sugeno (T-S) representation, and we recall the lateral forces proposed in [10] and [29] described as follows

$$\begin{aligned} &\text{if } |\,\alpha_f(t)\,| \text{ is } M_1 \text{ then } \begin{cases} F_{yf} = -C_{\alpha f1}\alpha_f(t); \\ F_{yr} = -C_{\alpha r1}\alpha_r(t), \end{cases} \\ &\text{if } |\,\alpha_f(t)\,| \text{ is } M_2 \text{ then } \begin{cases} F_{yf} = -C_{\alpha f2}\alpha_f(t); \\ F_{yr} = -C_{\alpha r2}\alpha_r(t), \end{cases} \end{aligned} \tag{5}$$

where $C_{\alpha fi}$ and $C_{\alpha ri}$ are the front and rear tire cornering stiffness coefficients, respectively, M_1 and M_2 are the fuzzy sets for slip angles. Using the membership function, the overall cornering forces (5) are described as following

$$\begin{aligned} F_{yf} &= -\sum_{i=1}^{2}\theta_i(|\,\alpha_f(t)\,|)C_{\alpha fi}\alpha_f(t), \\ F_{yr} &= -\sum_{i=1}^{2}\theta_i(|\,\alpha_f(t)\,|)C_{\alpha ri}\alpha_r(t), \end{aligned} \tag{6}$$

where the membership functions θ_i, $i = 1, 2$ satisfy the following conditions

$$\sum_{i=1}^{2}\theta_i(|\,\alpha_f(t)\,|) = 1, \ 0 \le \theta_i(|\,\alpha_f(t)\,|) \le 1, \quad i = 1, 2, \tag{7}$$

and are given by the following expression

$$\theta_i(|\,\alpha_f(t)\,|) = \frac{\omega_i(|\,\alpha_f(t)\,|)}{\sum_{i=1}^{2}\omega_i(|\,\alpha_f(t)\,|)}, \tag{8}$$

where $\omega_1(|\ \alpha_f(t)\ |)$ and $\omega_2(|\ \alpha_f(t)\ |)$ are membership functions given by

$$\omega_i(|\ \alpha_f(t)\ |) = \frac{1}{\left(1+\left|\frac{|\alpha_f(t)|-c_i}{d_i}\right|\right)^{2b_i}}. \tag{9}$$

Remark 1: To reduce the number of membership functions, the authors in [10] have considered $\alpha_f(t)$ and $\alpha_r(t)$ in the same fuzzy set. That is why the rules are only made for $\alpha_f(t)$, which in turn allows us to reduce the number of parameters to identify [30].

B. EXTERNAL FORCES

When the vehicles move and their velocity increases, it appears that external forces try to resist their movement, which may impact the protection requirements of the vehicle as a safety measure. Among these external forces we find the intensity of the wind, which is evident when the vehicle's velocity increases or when the weather changes. Assuming that the lateral force comprises an air resistance term, that is assumed to be a quadratic function of the lateral velocity of the vehicle $V_y(t)$, and using the T-S model given in (6), the lateral forces in (4) can be written as follows.

$$\begin{aligned} F_{yf} &= -\sum_{i=1}^{2}\theta_i(|\ \alpha_f(t)\ |)C_{\alpha fi}\alpha_f(t) - C_{Af}V_y^2(t), \\ F_{yr} &= -\sum_{i=1}^{2}\theta_i(|\ \alpha_f(t)\ |)C_{\alpha ri}\alpha_r(t) - C_{Ar}V_y^2(t). \end{aligned} \tag{10}$$

where C_{Af} and C_{Ar} are the front and rear air resistance coefficient, respectively.

Considering the relationship between the lateral velocity $V_y(t)$, the vehicle side-slip angle $\beta(t)$ and the longitudinal velocity $V_x(t)$, that is $\beta(t) = \frac{V_y(t)}{V_x(t)}$, (10) can be rewritten as

$$\begin{aligned} F_{yf} &= -\sum_{i=1}^{2}\theta_i(|\ \alpha_f(t)\ |)C_{\alpha fi}\alpha_f(t) - V_x^2(t)C_{Af}\beta^2(t), \\ F_{yr} &= -\sum_{i=1}^{2}\theta_i(|\ \alpha_f(t)\ |)C_{\alpha ri}\alpha_r(t) - V_x^2(t)C_{Ar}\beta^2(t). \end{aligned} \tag{11}$$

Remark 2: The vehicle model's complexity depends on the model of the cornering forces F_{yf} and F_{yr}. In the literature, several formulations have been proposed to define these forces. Moreover, these forces are given as a function of the tire slip angles using nonlinear relationships, as in [10], or as the form in (4). Furthermore, note that when $C_{Af} = C_{Ar} = 0$, (11) recovers the results presented in [10] and [29], which means that the front and rear tire forces proposed in this work are more general than the existing ones in the literature.

To obtain the coefficients defined in the membership parameters of the T–S model, we use the method cited in [10]. The obtained coefficients are described in Table 1.

C. TIME DELAYS

As discussed in [10], [21], [28] and [11], and the references therein, many works have considered both side-slip angles

TABLE 1. Parameters of the membership functions.

Parameters		Units
c_1= 0.0284	c_2= 0.1647	–
b_1= 1.7009	b_2=12.0064	–
d_1=0.0785	d_2= 0.1126	–
$C_{\alpha f1}$=55234	$C_{\alpha f2}$= 15544	N/m
$C_{\alpha r1}$= 49200	$C_{\alpha r2}$= 13543	N/m

$\beta_f(t)$ and $\beta_r(t)$, under the assumption that they are small. The relationship between them and the front and rear tire side-slip angles, $\alpha_f(t)$ and $\alpha_r(t)$, are given as follows

$$\begin{aligned} \alpha_f(t) &= \beta_f(t) - \delta(t) = \beta(t) + \frac{a_1}{V_x}\dot{\psi}(t) - \delta(t), \\ \alpha_r(t) &= \beta_r(t) = \beta(t) - \frac{a_2}{V_x}\dot{\psi}(t). \end{aligned} \tag{12}$$

Note that the approximation used to represent both side-slip angles is not unique and various approximations have been used in the literature. The assumption is unrealistic despite the representation used for the front and rear tire side-slip angles. In a practical setting, and when the vehicle's slip angle changes, the force system on the planar vehicle model can not respond immediately, which could translate into the presence of delays. Delays exist in many practical dynamical systems but are usually disregarded when designing controllers and observers. However, especially in safety-critical applications, they can be a source of performance and safety loss for the overall system, if they are not adequately addressed when synthetizing a controller or observer. Furthermore, since the vehicle should be safe for humans, it is essential to detect any possible problems that may arise due to its dynamical properties. For example, When a vehicle enters a turn, the lateral forces between the wheels and the roadway are proportional to the side-slip angle of the wheels. For a front-steered vehicle, the side-slip angle on the unsteered rear wheels takes a moment to build up, delaying the application of cornering forces to the rear wheels [25]. To improve the deficiencies of driver assistance systems, drawbacks in each system must be reduced or compensated. One such weakness is the delay required to generate adequate braking torque on a wheel brake [25]. This time delay of several tenths of a second is caused in part by the following factors [25]:

- Elasticities in the brake lines;
- The compressibility of the brake pads;
- Elasticities in the brake calipers.

Certain environmental conditions, such as heavy moisture and road salt buildup on the brake discs, can increase the time delay in the braking system.

Under the assumption that the equations of motion of the tire are stationary or at least quasi-stationary, we have that the introduced parameters, such as the values of circumferential slip, slip angle $\beta(t)$, camber angle, as well as the tire forces F_x, F_y, and tire torques M_z, remain constant over time or fluctuate very slowly [26]. These requirements are absent or insufficiently fulfilled to justify this assumption. In these

cases, the longitudinal slip and the side-slip angle ($\beta(t)$) change very fast with time, implying that the tire forces (F_x, F_y) and torques (M_z) can only build up with a time delay [26]. To consider the effect of the potential time-delay on the side slip angles, we consider the following representation of the front and rear tire side slip angles of the vehicle:

$$\begin{aligned}\alpha_f(t) &= l_1\beta(t) + (1-l_1)\beta(t-h(t)) + \frac{a_1}{V_x}\dot{\psi}(t) - \delta(t),\\ \alpha_r(t) &= l_2\beta(t) + (1-l_2)\beta(t-h(t)) - \frac{a_2}{V_x}\dot{\psi}(t),\end{aligned} \tag{13}$$

where l_1 and l_2 are delay parameters satisfying

$$0 \le l_1 \le 1 \ \text{ and } \ 0 \le l_2 \le 1 \tag{14}$$

and $h(t)$ is a time-varying delay satisfying the following constraint

$$0 \le h_1 \le h(t) \le h_2, \quad \dot{h}(t) \le \mu, \tag{15}$$

where h_1 and h_2 are the lower and upper bound of the time-varying delay, and μ is the upper bound of the time-varying delay derivative. Based on the above discussion, it can be concluded that the steering angles can be described by a delay while the yaw rate cannot.

Remark 3: The idea behind considering different delay parameters l_1 and l_2, as opposed to being equal, is that the front and rear side slip angles may not be affected by delays equally. Take for instance when a vehicle begins to navigate on irregular terrain (change of road conditions), or if the wheels are of different characteristics, or under an emergency situation (punctured wheel) or similar cases. Therefore, the proposed model is more general than the existing ones in the literature as it considers a potential delay parameter for the front side slip angle that may differ from the delay parameter for the rear side slip angle.

Remark 4: Notice that the time-delay tire side-slip angles given in (13) are more general than those provided in [21] and [10]. Thus, if $l_1 = l_2 = 1$ or ($h(t) = 0$) we obtain the delay-free tire side-slip angles as indicated in [21] and [10] and otherwise the tire side-slip angles are totally affected by delay. Moreover, the delay parameters l_1 and l_2 are the tuning parameters that help us introduce a delay in side-slip and yaw rate angles and allow us to control the percentage of the delay in the vehicle model.

A simple differential equation cannot successfully model many complex systems. For many systems, the future evolution of the state variables $x(t)$ depends not only on their current value of the state and its derivatives but also on their past values [31]. Furthermore, the delay is not just a mathematical concept; more significantly, it is embedded in many natural systems, such as biochemical reactions, industrial processes and mechatronic motions. Delay, as a universal part of many processes, is a phenomenon that undoubtedly deteriorates the quality of the control, causing oscillations and instability. Therefore, the stability and control analysis of such a system are of theoretical and practical importance. Considering a time-delay in the lateral vehicle model may allow us more information about the system's behavior, especially when these delays may be exacerbated in the event of an emergency or a change in road conditions.

Furthermore, the idea behind using (13) is to reconstruct the information that could be eliminated from the system when using the linear approximation in (3), which could affect the system's performance. Thus, the delayed part has been identified as global information, which is ignored when approximations are used.

It is assumed that the vehicle body moves at a constant forward speed, which means that $\dot{V}_x = 0$ and the first line in (1) becomes an independent algebraic equation. Therefore, the longitudinal force does not affect vehicle stability, and the integration into the system equation is unnecessary.

Combining (1), (10) and (13), and assuming the yaw rate $\dot{\psi}(t)$ as the output, the modelled vehicle system can be represented as follows:

$$\begin{aligned}\dot{x}(t) &= \sum_{i=1}^{2}\theta_i(|\ \alpha_f(t)\ |)\{A_i x(t) + A_{di}x(t-h(t)) \\ &\quad + B_i u(t)\} + f(x(t)),\\ y(t) &= \sum_{i=1}^{2}\theta_i(|\ \alpha_f(t)\ |)C_i x(t),\end{aligned} \tag{16}$$

where $x^T(t) = [x_1(t)\ \ x_2(t)] = [\beta(t)\ \ \dot{\psi}(t)]$ is the state vector and $\delta(t) = u(t)$ is the control input,

$$\begin{aligned}A_i &= \begin{bmatrix} -\pi_1^i & -(1+\pi_2^i) \\ -\pi_3^i & -\pi_4^i \end{bmatrix}, \quad B_i = \begin{bmatrix} 2\dfrac{C_{\alpha fi}}{mV_x} \\ 2\dfrac{a_1 C_{\alpha fi}}{I_z} \end{bmatrix},\\ f(x(t)) &= \begin{bmatrix} -\chi_1 x_1^2(t) \\ -\chi_3 x_1^2(t) \end{bmatrix}, \quad A_{di} = \begin{bmatrix} -\pi_5^i & 0 \\ -\pi_6^i & 0 \end{bmatrix},\\ C_i &= \begin{bmatrix} 0 & 1 \end{bmatrix},\end{aligned} \tag{17}$$

with

$$\begin{aligned}\pi_1^i &= 2\frac{l_1 C_{\alpha fi} + l_2 C_{\alpha ri}}{mV_x}, \quad \pi_2^i = 2\frac{a_1 C_{\alpha fi} - a_2 C_{\alpha ri}}{mV_x^2},\\ \pi_3^i &= 2\frac{a_1 l_1 C_{\alpha fi} - a_2 l_2 C_{\alpha ri}}{I_z}, \quad \pi_4^i = 2\frac{a_1^2 C_{\alpha fi} - a_2^2 C_{\alpha ri}}{I_z V_x},\\ \pi_5^i &= 2\frac{(1-l_1)C_{\alpha fi} + (1-l_2)C_{\alpha ri}}{mV_x},\\ \pi_6^i &= 2\frac{a_1(1-l_1)C_{\alpha fi} - a_2(1-l_2)C_{\alpha ri}}{I_z},\\ \chi_1 &= 2\frac{V_x(C_{Af} + C_{Ar})}{m}, \quad \chi_3 = 2\frac{(a_1 C_{Af} - a_2 C_{Ar})V_x^2}{I_z}.\end{aligned}$$

Remark 5: The lateral forces (11) depend not only on the tire side-slip angles but also on the vehicle side-slip angle. Because of this, we could recover the information ignored when using the approximation made in other works [10], [11], [21]. Moreover, by combining (13), the lateral forces (11) will be reformulated not only by the present vehicle side-slip but also by the side-slip from the past. Besides, as mentioned in Remark 4, the lateral forces (11) in combination

with (13) are reduced to those in [10], [21], and [11] when $h(t) = 0$ and $C_{Af} = C_{Ar} = 0$ or when $l_1 = l_2 = 1$ and $C_{Af} = C_{Ar} = 0$, which shows that the current model is more general.

The proposed vehicle system model in (16) is a nonlinear time-varying delay system, which is more general than some systems found in the literature. Moreover, since the nonlinear parts are of the kind x_1^2, they can be regarded as Lipschitz functions, at least locally, by considering that the operating range of x_1 is bounded. Because of that. in this work, it is assumed that the nonlinear function $f(x(t))$ satisfies the one-sided Lipschitz condition in [32], that is,

$$< f(x(t)), x(t) > \leq \rho_1 \parallel x(t) \parallel^2, \quad \rho_1 \in \mathbb{R}, \tag{18}$$

and also, verifies the quadratic inner-bounded condition given by

$$\parallel f(x(t)) \parallel^2 \leq \rho_2 \parallel x(t) \parallel^2 + \rho_3 < f(x(t)), x(t) > . \tag{19}$$

IV. OBSERVER-BASED CONTROL

As in many practical systems, the vehicle system states are not necessarily fully observable due to sensor and technology limitations or other practical reasons. Because of this, observer-based control is very relevant, as it seems to be well-suited for estimating the vehicle states from the measured vehicle output states. In this context, we will present the main results of this work by formulating an observer-based control problem for the proposed vehicle dynamics, followed by an LMI based approach for its design.

A. PROBLEM FORMULATION

In order to estimate the vehicle system states in (16), consider the following observer which has the same structure as the vehicle system:

$$\begin{aligned}
\dot{\bar{x}}(t) &= \sum_{i=1}^{2} \theta_i(\mid \alpha_f(t) \mid)\{A_i\bar{x}(t) + A_{di}\bar{x}(t - h(t)) \\
&\quad + B_i u(t) + L_i(y(t) - \bar{y}(t))\} + f(\bar{x}(t)), \\
u(t) &= \sum_{i=1}^{2} \theta_i(\mid \alpha_f(t) \mid)K_i\bar{x}(t), \\
\bar{y}(t) &= \sum_{i=1}^{2} \theta_i(\mid \alpha_f(t) \mid)C_i\bar{x}(t),
\end{aligned} \tag{20}$$

where $\bar{x}(t)$ is the state estimation of $x(t)$, $\bar{y}(t)$ is the observer output, and L_i and K_i are, respectively, the observer and the controller constant gain matrices.

Remark 6: Note that, the observer-based control given in (20) is more general than the traditional static-gain approach. The term $A_{di}\bar{x}(t - h(t))$ introduces a new degree of freedom to the system. In particular, assuming that $h(t) = 0$ and $A_{di} = 2L_iC_j$, system (20) is reduced to the conventional static-gain case.

The aim is to design the gains K_i and L_i such that the error defined as $e(t) = x(t) - \bar{x}(t)$ tends to zero in steady state. In order to achieve this, let us define the augmented error system as follows

$$\begin{aligned}
\dot{x}(t) &= A_k x(t) - B_k e(t) + A_d x(t - h(t)) + f(x(t)), \\
\dot{e}(t) &= A_L e(t) + A_d e(t - h(t)) + \Delta f(x(t), \bar{x}(t)).
\end{aligned} \tag{21}$$

where

$$\begin{aligned}
A_k &= \sum_{i=1}^{2}\sum_{j=1}^{2} \theta_i(\mid \alpha_f(t) \mid)\theta_j(\mid \alpha_f(t) \mid)(A_i + B_iK_j), \\
A_L &= \sum_{i=1}^{2}\sum_{j=1}^{2} \theta_i(\mid \alpha_f(t) \mid)\theta_j(\mid \alpha_f(t) \mid)(A_i - L_iC_j), \\
B_k &= \sum_{i=1}^{2}\sum_{j=1}^{2} \theta_i(\mid \alpha_f(t) \mid)\theta_j(\mid \alpha_f(t) \mid)(B_iK_j), \\
\Delta f(\bar{x}(t), x(t)) &= f(x(t)) - f(\bar{x}(t)).
\end{aligned} \tag{22}$$

Moreover, it is assumed that $\Delta f(x(t))$ verifies the one-sided Lipschitz and quadratic inner-bounded conditions described in the following conditions, for given scalars $\vartheta_i \in \mathbb{R}$, $i = 1, 2, 3$.

$$\begin{aligned}
< \Delta f(\bar{x}(t), x(t)), e(t) > &\leq \vartheta_1 \parallel e(t) \parallel^2 \\
\parallel \Delta f(\bar{x}(t), x(t)) \parallel^2 &\leq \vartheta_2 \parallel e(t) \parallel^2 \\
&\quad + \vartheta_3 < \Delta f(\bar{x}(t), x(t)), e(t) > .
\end{aligned} \tag{23}$$

One can see that the error goes to zero when the time-delay system (21) is asymptotically stable. The notation in (22) is used to help us in the development of our results.

Most of the works in the literature that study time-delay systems use the boundedness of integral terms, since these terms appear in the time-derivative of a Lyapunov-Krasovskii functional. In recent years, a significant reduction in the conservatism of stability results has been achieved due to the boundedness of these terms and the use of Wirtinger's inequality (Lemma 1). Next, we present two technical lemmas that are helpful when deriving our results.

Lemma 1 [16]: For any matrix $R > 0$, and a differentiable signal $x \in [h_1, h_2] \to \mathbb{R}^n$, the following inequality holds:

$$-\int_{h_1}^{h_2} \dot{x}^T(s)R\dot{x}(s)ds \leq \frac{1}{h_2 - h_1}\xi^T\Phi(R)\xi, \tag{24}$$

where $\xi = [x^T(h_2) \;\; x^T(h_1) \;\; \frac{1}{h_2-h_1}\int_{h_1}^{h_2} x^T(s)ds]^T$ and

$$\Phi(R) = \begin{bmatrix} -4R & -2R & 6R \\ * & -4R & 6R \\ * & * & -12R \end{bmatrix}. \tag{25}$$

Lemma 2 [33]: For matrices V, L and $Z > 0$ with appropriate dimensions, the following inequality holds:

$$\mathrm{VL} + \mathrm{L}^T\mathrm{V}^T \leq \mathrm{V}\epsilon\mathrm{Z}\mathrm{V}^T + \mathrm{L}^T(\epsilon\mathrm{Z})^{-1}\mathrm{L}. \tag{26}$$

B. TIME-DELAY OBSERVER-BASED CONTROL DESIGN

Now, we consider a time-delay observer-based control to estimate the vehicle model states developed in the above section and to ensure that the closed-loop system is asymptotically stable. Additionally, we consider that the controller gains are

known and, based on the Lyapunov-Krasovskii functional, we present the condition that ensures the stability of system (21). First we have the following result.

Theorem 1: Let us consider the system (16), with conditions (18), (19), and (23) satisfied, and the proposed observer in (20) with given gains K_i and L_i, $i = 1, 2$. The augmented time-varying delay error system in (21) is asymptotically stable, with given gains K_i and L_i, if for given positive scalars γ_1, γ_2 , there exist positive definite matrices Q_r, N_r, $r = 1, 2, 3$, $diag\{P_{x11}, P_{x22}, P_{x33}\}$, R_1, R_2, T_1, T_2, $diag\{P_{e11}, P_{e22}, P_{e33}\}$, and positive scalars γ_3 and γ_4 such that the following conditions hold

$$\Omega_{ij} < 0, \quad i, j = 1, 2, \tag{27}$$

where

$$\Omega_{ij} = \begin{bmatrix} \Omega_x^{ij} & \Omega_{xe}^{ij} \\ * & \bar{\Omega}_e^{ij} \end{bmatrix} + \begin{bmatrix} \Gamma_{1ij}^T \\ \Gamma_{2ij}^T \end{bmatrix} (h_1^2 R_1 + h_{12}^2 R_2) \begin{bmatrix} \Gamma_{1ij}^T \\ \Gamma_{2ij}^T \end{bmatrix}^T, \tag{28}$$

with h_{12}, $\bar{\Omega}_e^{ij}$, Ω_x^{ij}, and Ω_e^{ij}, as shown in the equation at the bottom of the page.

$$\begin{aligned}
\Omega_{x11}^{ij} &= sym\{P_{x11}A_k^{ij}\} + Q_1 + 2\sigma_1 I - 4R_1, \\
\Omega_{x15} &= h_1 P_{x22} + 6R_1, \\
\Omega_{x17} &= P_{x11} + 2\sigma_2 I, \\
\Omega_{x22} &= -(Q_1 - Q_2) - 4R_1 - 4R_2, \\
\Omega_{x25} &= -h_1 P_{x22} + 6R_1, \\
\Omega_{x26} &= h_{12} P_{x33} + 6R_2, \\
\Omega_{x33} &= -(1-\mu)(Q_2 - Q_3), \\
\Omega_{x44} &= -Q_3 - 4R_2, \\
\Omega_{x46} &= -h_{12} P_{x33} + 6R_2, \\
\sigma_1 &= \gamma_1\rho_1 + \gamma_2\rho_2, \ \sigma_2 = \gamma_2\rho_3 - \gamma_1, \\
\Omega_{e11}^{ij} &= sym\{P_{e11}A_L^{ij}\} + N_1 + 2\sigma_3 I - 4T_1, \\
\Omega_{e15} &= h_1 P_{e22} + 6T_1, \\
\Omega_{e17} &= P_{e11} + 2\sigma_4 I, \\
\Omega_{e22} &= -(N_1 - N_2) - 4T_1 - 4T_2, \\
\Omega_{e25} &= -h_1 P_{e22} + 6T_1, \\
\Omega_{e26} &= h_{12} P_{e33} + 6T_2, \\
\Omega_{e33} &= -(1-\mu)(N_2 - N_3), \\
\Omega_{e44} &= -N_3 - 4T_2, \\
\Omega_{e46} &= -h_{12} P_{e33} + 6T_2, \\
\sigma_3 &= \gamma_3\vartheta_1 + \gamma_4\vartheta_2, \quad \sigma_4 = \gamma_4\vartheta_3 - \gamma_3, \\
\Omega_{xe}^{ij} &= \begin{bmatrix} -P_{x11}B_k^{ij} & \mathbf{0_{n\times 6n}} \\ \mathbf{0_{6n\times n}} & \mathbf{0_{6n\times 6n}} \end{bmatrix}, \\
\Gamma_{1ij} &= \begin{bmatrix} A_k^{ij} & 0 & A_d^i & \mathbf{0_{n\times 3n}} & I_n \end{bmatrix}, \\
\Gamma_{2ij} &= \begin{bmatrix} -B_k^{ij} & \mathbf{0_{n\times 6n}} \end{bmatrix}, \\
\Pi_{2ij} &= \begin{bmatrix} A_L^{ij} & 0 & A_d^i & \mathbf{0_{n\times 3n}} & I_n \end{bmatrix}.
\end{aligned}$$

Proof: See Appendix A.

Theorem 1 was obtained by using Wirtinger's inequality (Lemma 1) [16], which has been shown to reduce conservatism on the related bounds when compared to using Jensen's inequality.

Notice that Theorem 1 provides a delay-dependent stability analysis of the lateral vehicle described in (1). Moreover, the conditions presented in Theorem 1 are linear for given controller gains K_i and L_i. Thus, they can be solved in a straightforward manner using the standard LMI-Toolbox solver [34].

If the controller gains K_i and L_i are variable, we have that condition (27) is not an LMI, since nonlinear terms will appear. Therefore, more work is required to solve the nonlinearity problem in Theorem 1. The following theorem presents sufficient conditions to design both gains K_i and L_i simultaneously, in order to ensure the asymptotic stability of the closed-loop system (21).

$$\begin{aligned}
h_{12} &= h_2 - h_1, \\
\bar{\Omega}_e^{ij} &= \Omega_e^{ij} + \Pi_{2ij}^T (h_1^2 T_1 + h_{12}^2 T_2) \Pi_{2ij}, \\
\Omega_x^{ij} &= \begin{bmatrix}
\Omega_{x11}^{ij} & -2R_1 & P_{x11}A_d^i & 0 & \Omega_{x15} & 0 & \Omega_{x17} \\
* & \Omega_{x22} & 0 & -2R_2 & \Omega_{x25} & \Omega_{x26} & 0 \\
* & * & \Omega_{x33} & 0 & 0 & 0 & 0 \\
* & * & * & \Omega_{x44} & 0 & \Omega_{x46} & 0 \\
* & * & * & * & -12R_1 & 0 & 0 \\
* & * & * & * & * & -12R_2 & 0 \\
* & * & * & * & * & * & -2\gamma_2 I
\end{bmatrix}, \\
\Omega_e^{ij} &= \begin{bmatrix}
\Omega_{e11}^{ij} & -2T_1 & P_{e11}A_d^i & 0 & \Omega_{e15} & 0 & \Omega_{e17} \\
* & \Omega_{e22} & 0 & -2T_2 & \Omega_{e25} & \Omega_{e26} & 0 \\
* & * & \Omega_{e33} & 0 & 0 & 0 & 0 \\
* & * & * & \Omega_{e44} & 0 & \Omega_{e46} & 0 \\
* & * & * & * & -12T_1 & 0 & 0 \\
* & * & * & * & * & -12T_2 & 0 \\
* & * & * & * & * & * & -2\gamma_4 I
\end{bmatrix},
\end{aligned}$$

Theorem 2: System (16) is asymptotically stabilizable by (20) if for given positive scalars γ_1, γ_2, there exist positive definite matrices $\tilde{Q}_r$, N_r, $r = 1, 2, 3$, $diag\{X_{11}, \tilde{P}_{x22}, \tilde{P}_{x33}\}$, $diag\{P_{e11}, P_{e22}, P_{e33}\}$, $\tilde{R}_1$, $\tilde{R}_2$, T_1, T_2, matrices Y_i, G_i and positive scalars γ_3 and γ_4 such that the following conditions hold

$$\Xi_{ii} < 0, \quad i = 1, 2, \tag{29}$$

$$\Xi_{ij} + \Xi_{ji} < 0, \quad 1 \leq i < j \leq 2, \tag{30}$$

where h_{12}, Ξ_{ij}, $\bar{\Omega}_{ij}(0)$, $\tilde{\Omega}_x^{ij}$, and Ω_e^{ij}, as shown in the equation at the bottom of the page.

$$\begin{aligned}
\tilde{\mathfrak{I}}_1 &= T_1 - 2P_{e11},\\
\tilde{\mathfrak{I}}_2 &= T_2 - 2P_{e11},\\
\tilde{\mathfrak{I}}_1 &= \tilde{R}_1 - 2X_{11},\\
\tilde{\mathfrak{I}}_2 &= \tilde{R}_2 - 2X_{11},\\
\tilde{\Omega}_{x11}^{ij} &= sym\{A_iX_{11} + B_iY_j\} + \tilde{Q}_1 + 2\sigma_1X_{11}X_{11} - 4\tilde{R}_1,\\
\tilde{\Omega}_{x15} &= h_1\tilde{P}_{x22} + 6\tilde{R}_1,\\
\tilde{\Omega}_{x17} &= X_{11} + 2\sigma_2X_{11},\\
\tilde{\Omega}_{x22} &= -(\tilde{Q}_1 - \tilde{Q}_2) - 4\tilde{R}_1 - 4\tilde{R}_2,\\
\tilde{\Omega}_{x25} &= -h_1\tilde{P}_{x22} + 6\tilde{R}_1,\\
\tilde{\Omega}_{x26} &= h_{12}\tilde{P}_{x33} + 6\tilde{R}_2,\\
\tilde{\Omega}_{x33} &= -(1-\mu)(\tilde{Q}_2 - \tilde{Q}_3),\\
\tilde{\Omega}_{x44} &= -\tilde{Q}_3 - 4\tilde{R}_2,\\
\tilde{\Omega}_{x46} &= -h_{12}\tilde{P}_{x33} + 6\tilde{R}_2,\\
\sigma_1 &= \gamma_1\rho_1 + \gamma_2\rho_2,\\
\sigma_2 &= \gamma_2\rho_3 - \gamma_1,\\
\Omega_{e11}^{ij} &= sym\{P_{e11}A_i - G_iC_j\} + N_1 + 2\sigma_3 I - 4T_1,\\
\bar{\mathrm{V}}_{ij} &= \begin{bmatrix}(B_iY_j)^T & \mathbf{0}_{n\times 15n} & h_1(B_iY_j)^T & h_{12}(B_iY_j)^T\end{bmatrix}^T,\\
\tilde{\Gamma}_{1ij}^T &= \begin{bmatrix}A_iX_{11} + B_iY_j & 0 & A_{di}X_{11} & \mathbf{0_{n\times 3n}} & I_n\end{bmatrix}^T,\\
\mathrm{L} &= \begin{bmatrix}\mathbf{0}_{n\times 7n} & \mathbf{I} & \mathbf{0}_{n\times 4n}\end{bmatrix}.
\end{aligned}$$

Moreover, if the above conditions are satisfied, the parameters of the observer-based controller are obtained as follows

$$K_i = Y_iX_{11}^{-1}, \quad L_i = P_{e11}^{-1}G_i. \tag{31}$$

Proof: The proof can be found in Appendix B.

Theorem 2 provides a new design methodology for both controller and observer gains simultaneously. The design methodology has been developed without structural restrictions on the Lyapunov matrices, which reduces conservatism. The obtained controller and observer gains ensure that the closed-loop vehicle system is asymptotically stable for all admissible delays.

Remark 7: To get less restrictive conditions for the control and observer gains design, a new matrix variable is introduced in Theorem 2 in order to separate the dynamical system matrices from the Lyapunov matrix. This delivers the condition (51), which is not linear for a given scalar ϵ. Several

$$\begin{aligned}
h_{12} &= h_2 - h_1,\\
\Xi_{ij} &= \begin{bmatrix}\bar{\Omega}_{ij}(0) & \bar{\mathrm{V}}_{ij} & \mathrm{L}^T\\ * & -(2\delta_1 - \delta_2)I & 0\\ * & * & -\delta_2 I\end{bmatrix},\\
\bar{\Omega}_{ij}(0) &= \begin{bmatrix}\tilde{\Omega}_x^{ij} & \mathbf{0_{7n\times 7n}} & \mathbf{0_{7n\times n}} & \mathbf{0_{7n\times n}} & h_1\tilde{\Gamma}_{1ij}^T & h_{12}\tilde{\Gamma}_{1ij}^T\\ * & \Omega_e^{ij} & h_1\Pi_{2ij}^TP_{e11} & h_{12}\Pi_{2ij}^TP_{e11} & \mathbf{0_{7n\times n}} & \mathbf{0_{7n\times n}}\\ * & * & \tilde{\mathfrak{I}}_1 & \mathbf{0_{n\times n}} & \mathbf{0_{n\times n}} & \mathbf{0_{n\times n}}\\ * & * & * & \tilde{\mathfrak{I}}_2 & \mathbf{0_{n\times n}} & \mathbf{0_{n\times n}}\\ * & * & * & * & \tilde{\mathfrak{I}}_1 & \mathbf{0_{n\times n}}\\ * & * & * & * & * & \tilde{\mathfrak{I}}_2\end{bmatrix},\\
\tilde{\Omega}_x^{ij} &= \begin{bmatrix}\tilde{\Omega}_{x11}^{ij} & -2\tilde{R}_1 & A_{di}X_{11} & \mathbf{0_{n\times n}} & \tilde{\Omega}_{x15} & \mathbf{0_{n\times n}} & \tilde{\Omega}_{x17}\\ * & \tilde{\Omega}_{x22} & \mathbf{0_{n\times n}} & -2\tilde{R}_2 & \tilde{\Omega}_{x25} & \tilde{\Omega}_{x26} & \mathbf{0_{n\times n}}\\ * & * & \tilde{\Omega}_{x33} & \mathbf{0_{n\times n}} & \mathbf{0_{n\times n}} & \mathbf{0_{n\times n}} & \mathbf{0_{n\times n}}\\ * & * & * & \tilde{\Omega}_{x44} & \mathbf{0_{n\times n}} & \tilde{\Omega}_{x46} & \mathbf{0_{n\times n}}\\ * & * & * & * & -12\tilde{R}_1 & \mathbf{0_{n\times n}} & \mathbf{0_{n\times n}}\\ * & * & * & * & * & -12\tilde{R}_2 & \mathbf{0_{n\times n}}\\ * & * & * & * & * & * & -2\gamma_2 I\end{bmatrix},\\
\Omega_e^{ij} &= \begin{bmatrix}\Omega_{e11}^{ij} & -2T_1 & P_{e11}A_{di} & \mathbf{0_{n\times n}} & \Omega_{e15} & \mathbf{0_{n\times n}} & \Omega_{e17}\\ * & \Omega_{e22} & \mathbf{0_{n\times n}} & -2T_2 & \Omega_{e25} & \Omega_{e26} & \mathbf{0_{n\times n}}\\ * & * & \Omega_{e33} & \mathbf{0_{n\times n}} & \mathbf{0_{n\times n}} & \mathbf{0_{n\times n}} & \mathbf{0_{n\times n}}\\ * & * & * & \Omega_{e44} & \mathbf{0_{n\times n}} & \Omega_{e46} & \mathbf{0_{n\times n}}\\ * & * & * & * & -12T_1 & \mathbf{0_{n\times n}} & \mathbf{0_{n\times n}}\\ * & * & * & * & * & -12T_2 & \mathbf{0_{n\times n}}\\ * & * & * & * & * & * & -2\gamma_4 I\end{bmatrix},
\end{aligned}$$

researchers have explored how to choose this scalar, and several methods have been developed to find the optimal scalar, namely *fminsearch*. To overcome the complexity of choosing ϵ, we implement the inequality $X_{11} > \delta_1 I$ by means of the inequality $-\frac{1}{\epsilon} \leq -(2-\epsilon)$. These inequalities help us deal with the nonlinearity set out in (51) and allow us to obtain the LMI conditions (29) and (30).

V. SIMULATION RESULTS

To illustrate the efficacy of the proposed methodology to obtain the gains of the fuzzy observer-based control to estimate the vehicle state, we use the vehicle parameters [10], [30] given in Table 2 and the membership parameters [10] given in Table 1.

TABLE 2. Vehicle parameters.

Parameter	Value	Unit
V_x	80	$m.s^{-1}$
I_z	2988	$Kg.m^2$
a_1	1.18	m
a_2	1.77	m
m	1832	Kg

First, we will demonstrate the impact of the function $f(x(t))$ and the time-varying delay on the side-slip and yaw rate angles by perturbing the vehicle model with the delay $h(t)$ with different delay parameters $l_1 \neq l_2$ and with $l_1 = l_2$. Consider an input signal $\delta(t) = 0.3$, $C_{Af} = C_{Ar} = 0.5$, $0.1 \leq h(t) \leq 0.7$, $\mu = 0.3$ and the following initial condition $x(0) = [0 \;\; 0]^T$. The side-slip angles are plotted in Fig. 2 for $l_1 \neq 1$ or $l_2 \neq 1$ (delayed side-slip angle) and for $l_1 = l_2 = 1$ (delay-free side-slip angle). The yaw rate angles are plotted in Fig. 3 for $l_1 \neq 1$ or $l_2 \neq 1$ (delayed yaw rate angle) and for $l_1 = l_2 = 1$ (delay-free yaw rate angle).

According to Fig. 2 and Fig. 3, the time-varying delay and nonlinear dynamics have a significant impact on the side-slip and yaw-rate angles, as large oscillations occur when the time-varying delay becomes meaningful. Furthermore, it can be seen that when the delay is high in the vehicle states (side-slip and yaw-rate angles), it can cause destabilization and performance degradation. Additionally, when $l_1 = l_2 = 1$, which means that the system states are delay-free, one can see the effect of the nonlinearity $f(x(t))$ on the vehicle states. This demonstrates the significance of including the possible appearance of a delay in the vehicle model states.

We now consider the delay parameters as $l_1 = 0.5$ and $l_2 = 0.7$. The time-varying delay $h(t)$ as $0.1 \leq h(t) \leq 0.6$ which means that $h_1 = 0.1$ and $h_2 = 0.6$ and $\mu = 0.3$. Applying Theorem 2, the observer and controller gains obtained for $\gamma_1 = 2$, $\rho_1 = -0.9$, $\gamma_2 = 5$, $\rho_2 = 0.7$, $\rho_3 = -0.15$, $\vartheta_1 = 0.09$, $\vartheta_2 = 0.9$, $\vartheta_3 = 0.05$ are given by.

$$\left[\begin{array}{c|c} K_1 & L_1 \\ \hline K_2 & L_2 \end{array}\right] = \left[\begin{array}{c|c} [-0.3876 \quad -0.1719] & \begin{bmatrix} 0.4935 \\ 12.8226 \end{bmatrix} \\ \hline [-0.1279 \;\; -0.4106] & \begin{bmatrix} 0.6128 \\ 7.8630 \end{bmatrix} \end{array}\right]. \tag{32}$$

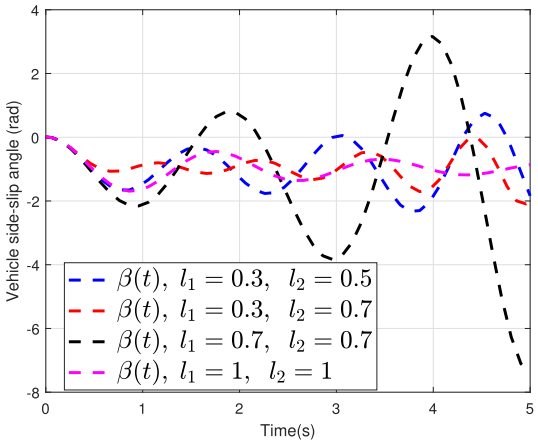

FIGURE 2. Vehicle side-slip angles.

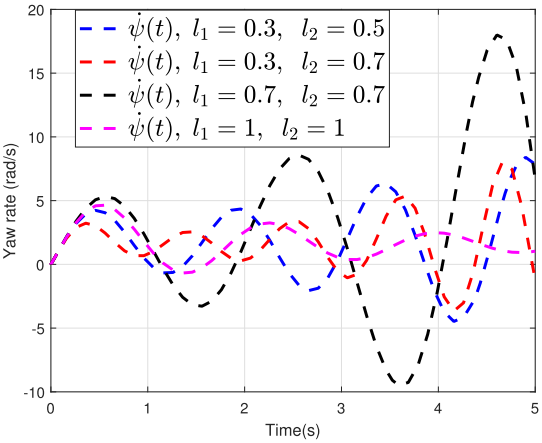

FIGURE 3. Yaw rate angles.

To demonstrate the effectiveness of the proposed approach, we will disturb the vehicle system with time-varying delay, and we will use the observer-based control scheme with gains (32) to estimate the vehicle states $\beta(t)$ and $\dot{\psi}(t)$. The vehicle side-slip $\beta(t)$ and yaw rate $\dot{\psi}(t)$ angles over time are displayed in Fig. 4 and Fig. 5, respectively. Fig. 4 shows the trajectory of the side-slip angle $\beta(t)$ and its estimate $\bar{\beta}(t)$, while Fig. 5 shows the trajectory of the yaw rate angle $\dot{\psi}(t)$ and its estimate $\dot{\bar{\psi}}(t)$. These simulations were obtained by using the initial conditions $x(0) = 0$ and $\bar{x}(0) = [-0.1\pi \;\; 0.3\pi]^T$. The time-varying delay is chosen as $h(t) = 0.1 + 0.5 \mid \sin 0.6t \mid$.

From Fig 4 and Fig 5, we can see that the estimation of the vehicle's state with a small-amplitude converges to the system states after 1 *second* for the side-slip angle and before 1 *second* for the yaw rate angle. The estimation is inaccurate before 1 *second*. This can occur for several reasons, for instance, the initial conditions, the time-varying delay, the nonlinear function $f(x(t))$, and the dynamics not included in the mathematical model. As a result, the estimation becomes significant and successful after 1 *second* for side-slip and yaw rate angles. Moreover, the effect of the delay can be seen in the trajectory of the vehicle states where the oscillation has

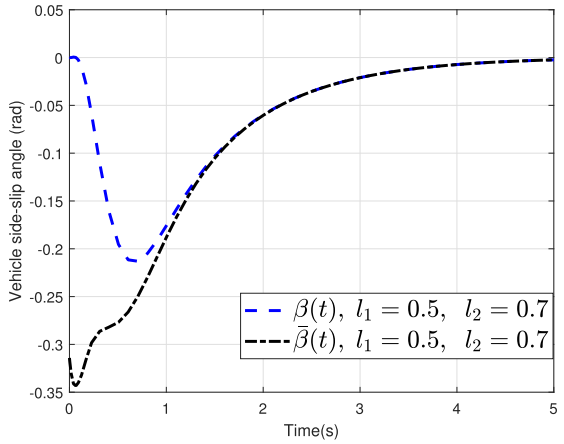

FIGURE 4. Side-slip angle and its estimate.

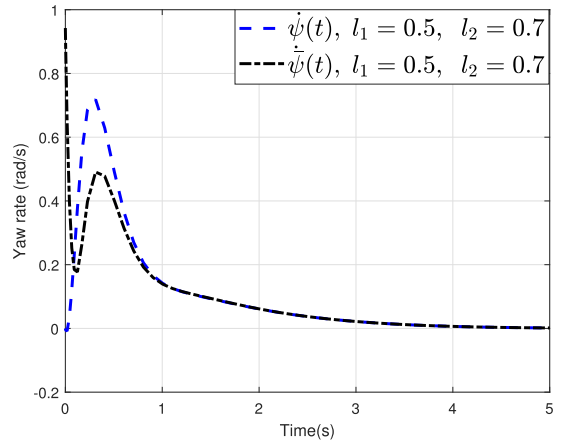

FIGURE 5. Yaw rate angle and its estimate.

arisen. Finally, the system states are asymptotically stable using the controller gains (32).

In the case where $l_1 = 1$ and $l_2 = 1$, which means that $A_{di} = 0,\ \ i = 1, 2$ and by applying Theorem 2, the observer-based controller gains for (20) are given by

$$\left[\begin{array}{c|c} K_1 & L_1 \\ \hline K_2 & L_2 \end{array}\right] = \left[\begin{array}{c|c} [-0.3099 \quad -0.1520] & \begin{bmatrix} 0.4002 \\ 10.4119 \end{bmatrix} \\ \hline \begin{bmatrix} -0.1553 & -0.3771 \end{bmatrix} & \begin{bmatrix} 0.2835 \\ 6.3246 \end{bmatrix} \end{array}\right]. \tag{33}$$

Fig 6 and Fig 7 display the vehicle states for the delay-free model and for the standard observer-based control structure with $l_1 = 1$ and $l_2 = 1$. The simulation was performed with the controller gains (33) and the initial conditions $x(0) = 0$ and $\bar{x}(0) = [-0.1\pi \quad 0.3\pi]^T$.

For comparison purposes, in Fig 6 and Fig 7, we can see that the vehicle states and their estimates converge to zero, implying that they are asymptotically stable when using the delay-free observer.

To show the efficiency of the control structures, $A_d \neq 0$ with the controller gains in (32), and $A_d = 0$ (standard control structure) with the controller gains in (33), we perturb the

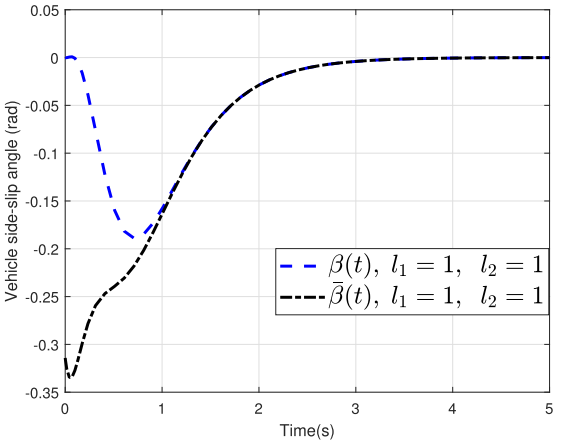

FIGURE 6. Side-slip angle and its estimate for $l_1 = 1$.

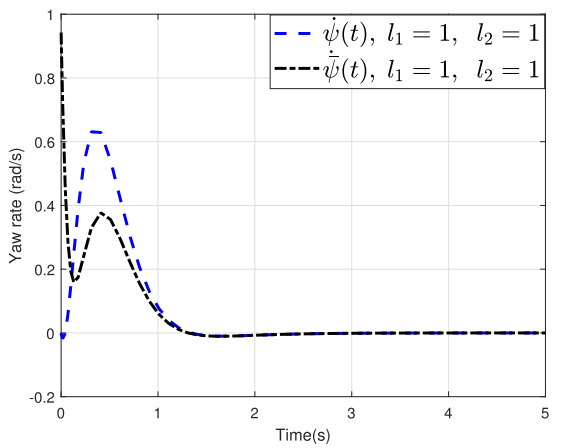

FIGURE 7. Yaw rate angle and its estimate for $l_1 = 1$.

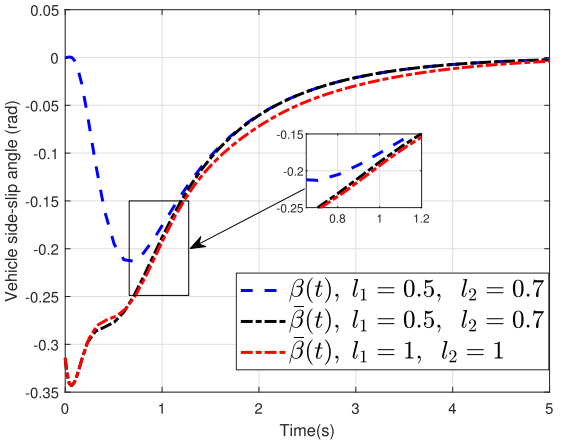

FIGURE 8. Vehicle side-slip angle and its estimate.

vehicle model with a time-varying delay and use the two control structures to estimate the vehicle states. The initial conditions used for the simulation are $x(0) = 0$ and $\bar{x}(0) = [-0.1\pi \quad 0.3\pi]^T$, and the time-varying delay considered is $h(t) = 0.1 + 0.5 \mid \sin 0.6t \mid$. The vehicle side-slip and yaw rate angles and their estimates are displayed in Fig. 8 and Fig 9, respectively.

It is evident from Fig. 8 that the standard control scheme $A_d = 0$ does not estimate the vehicle side-slip angle $\beta(t)$ when the time-varying delay occurs. While the proposed control scheme $A_d \neq 0$ provides a good estimation of the vehicle state. This illustrates the efficacy of the proposed control scheme in the presence of time-varying delays and nonlinear dynamics.

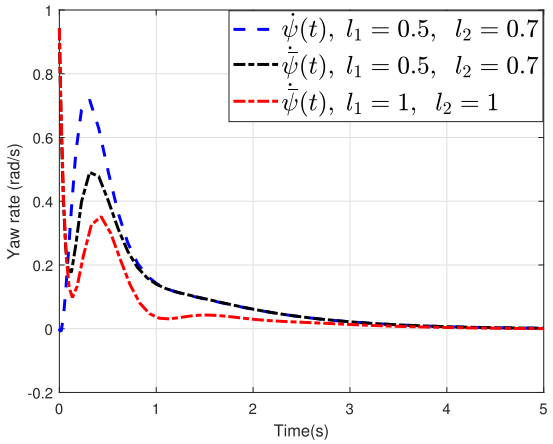

FIGURE 9. Yaw rate angle and its estimate.

Fig. 9 shows that the proposed control scheme ($A_d \neq 0$) is successful in estimating the vehicle states while the standard control scheme $A_d = 0$ offers defective estimation of the yaw rate $\dot{\psi}(t)$. We can infer from these results that the efficiency given by the proposed control structure is better than that provided by the traditional control scheme. This has been demonstrated by comparing the state estimation of the standard control scheme and the proposed scheme. We can also see that the gains obtained can control the vehicle system. Finally, these results highlight the importance of considering the presence of a delay in such systems.

VI. DISCUSSION

The lateral vehicle model, widely used in vehicle dynamics, offers a detailed representation of chassis motion [10], [11], [21], [22], [24]. In particular, [23] had proposed an extended representation of the vehicle model considering roll, which yields better results. Note that, in comparison to the proposed lateral vehicle model, the aforementioned model is a special case when $l_1 = l_2 = 1$ (or $h(t) = 0$). Since the lateral vehicle models found in the literature are delay-free [10], [11], [21], [22], [24], [35], a direct comparison with the proposed time delay model may be unfair. Because of that, a general comparison in terms of time-varying delay may be more significant, and it is done in this paper, where a delay-free lateral model and a time-varying delay lateral vehicle model have been compared in Section V.

VII. CONCLUSION

In this work, we developed a time-delay vehicle model using a simple formula that helps us introduce a time-varying delay in its states and considering that the lateral vehicle's air resistance can be represented as a Lipschitz function. The global nonlinear vehicle model was represented by a fuzzy T-S model with a time-varying delay and stability conditions were obtained based on an appropriate Lyapunov-Krasovskii functional in combination with Wirtinger's inequality.

The vehicle side-slip and yaw rate angles were estimated using a T-S observer-based control with a time-varying delay. The observer and controller gains have been designed simultaneously using a new design methodology formulated in terms of linear matrix inequalities. Numerical simulations showed a clear benefit of considering a model with delays as the control scheme without it underperforms when it is used to control the delayed system. In contrast, the proposed approach can estimate the vehicle states better and stabilize its dynamics. Future work could focus on full vehicle models with time-varying parameters and delays.

CONFLICT OF INTEREST

The authors declare that they have no conflict of interest.

APPENDIX A
PROOF OF THEOREM 1

Let us consider the following Lyapunov-Krasovskii functional

$$V(x(t), e(t)) = V_1(x(t)) + V_2(e(t)), \tag{34}$$

where

$$\begin{aligned} V_1(x(t)) = {} & \eta_x^T(t) P_d^x \eta_x(t) + \int_{t-h_1}^{t} x^T(s) Q_1 x(s) ds \\ & + \int_{t-h(t)}^{t-h_1} x^T(s) Q_2 x(s) ds \\ & + \int_{t-h_2}^{t-h(t)} x^T(s) Q_3 x(s) ds \\ & + h_1 \int_{-h_1}^{0} \int_{t+\lambda}^{t} \dot{x}^T(s) R_1 \dot{x}(s) ds d\lambda \\ & + h_{12} \int_{-h_2}^{-h_1} \int_{t+\lambda}^{t} \dot{x}^T(s) R_2 \dot{x}(s) ds d\lambda, \end{aligned} \tag{35}$$

$$\begin{aligned} V_2(e(t)) = {} & \eta_e^T(t) P_d^e \eta_e(t) + \int_{t-h_1}^{t} e^T(s) N_1 e(s) ds \\ & + \int_{t-h(t)}^{t-h_1} e^T(s) N_2 e(s) ds \\ & + \int_{t-h_2}^{t-h(t)} e^T(s) N_3 e(s) ds \\ & + h_1 \int_{-h_1}^{0} \int_{t+\lambda}^{t} \dot{e}^T(s) T_1 \dot{e}(s) ds d\lambda \\ & + h_{12} \int_{-h_2}^{-h_1} \int_{t+\lambda}^{t} \dot{e}^T(s) T_2 \dot{e}(s) ds d\lambda, \end{aligned} \tag{36}$$

with

$$\begin{aligned} & h_{12} = h_2 - h_1, \\ & \eta_{\oslash}^T = [\oslash(t) \ (\int_{t-h_1}^{t} \oslash(s) ds)^T \ (\int_{t-h_2}^{t-h_1} \oslash(s) ds)^T], \\ & P_d^{\oslash} = diag\{P_{\oslash 11}, P_{\oslash 22}, P_{\oslash 33}\}, \quad \oslash = \{x, e\}. \end{aligned}$$

Taking the derivative of $V_1(x(t))$ along the trajectory of $x(t)$, we obtain

$$\begin{aligned}\dot{V}_1(x(t)) \le\ & \eta_x^T(t)P_d^x\dot{\eta}_x(t) + x^T(t)Q_1x(t)\\ & - x^T(t-h_1)(Q_1-Q_2)x(t-h_1)\\ & -(1-\mu)x^T(t-h(t))(Q_2-Q_3)x(t-h(t))\\ & - x^T(t-h_2)Q_3x(t-h_2)\\ & + \dot{x}^T(t)(h_1^2R_1+h_{12}^2R_2)\dot{x}(t)\\ & - h_1\int_{t-h_1}^{t}\dot{x}^T(s)R_1\dot{x}(s)ds\\ & - h_{12}\int_{t-h_2}^{t-h_1}\dot{x}^T(s)R_2\dot{x}(s)ds. \end{aligned} \tag{37}$$

Using Lemma 1 for the last two integral terms, one can obtain

$$\begin{aligned} -h_1\int_{t-h_1}^{t}\dot{x}^T(s)R_1\dot{x}(s)ds &\le \xi^T\Phi(R_1)\xi,\\ -h_{12}\int_{t-h_2}^{t-h_1}\dot{x}^T(s)R_2\dot{x}(s)ds &\le \xi^T\Phi(R_2)\xi. \end{aligned} \tag{38}$$

Condition (18) implies that there exists a $\gamma_1 > 0$ such that.

$$2\gamma_1\{\rho_1x^T(t)x(t) - f^T(x(t))x(t)\} \ge 0. \tag{39}$$

We also note that (19) implies that there exists a $\gamma_2 > 0$ such that

$$2\gamma_2\{\rho_2x^T(t)x(t) + \rho_3f^T(x(t))x(t) - f^T(x(t))f(x(t))\} \ge 0. \tag{40}$$

Substituting (38) into (37) in combination with (39) and (40), we obtain

$$\begin{aligned}\dot{V}_1(x(t)) \le & \begin{bmatrix}\zeta_x\\ e(t)\end{bmatrix}^T\left\{\begin{bmatrix}\Omega_x & \begin{bmatrix}-P_{x11}B_k\\ \mathbf{0}_{6n\times n}\end{bmatrix}\\ * & 0\end{bmatrix}\right.\\ & \left. + \Pi_1^T(h_1^2R_1+h_{12}^2R_2)\Pi_1\right\}\begin{bmatrix}\zeta_x\\ e(t)\end{bmatrix}, \end{aligned} \tag{41}$$

where

$$\begin{aligned}\zeta_x^T &= [x^T(t)\ x^T(t-h_1)\ x^T(t-h(t))\ x^T(t-h_2)\\ &\quad \times \varphi_1^T\ \varphi_2^T\ f^T(x(t))],\\ \varphi_1^T &= (\frac{1}{h_1}\int_{t-h_1}^{t}x(s)ds)^T,\quad \varphi_2^T = (\frac{1}{h_{12}}\int_{t-h_2}^{t-h_1}x(s)ds)^T\\ \Pi_1 &= \begin{bmatrix}A_k & 0 & A_d & \mathbf{0_{n\times 3n}} & I_n & -B_k\end{bmatrix}. \end{aligned}$$

The time derivative of $V_2(e(t))$ along the trajectory of $e(t)$ can be obtained by following a similar approach as in the derivative for $V_1(x(t))$

$$\begin{aligned}\dot{V}_2(e(t)) \le\ & \eta_e^T(t)P_d^e\dot{\eta}_e(t) + e^T(t)N_1e(t)\\ & - e^T(t-h_1)(N_1-N_2)e(t-h_1)\\ & -(1-\mu)e^T(t-h(t))(N_2-N_3)e(t-h(t))\\ & - e^T(t-h_2)N_3e(t-h_2)\\ & + \dot{e}^T(t)(h_1^2T_1+h_{12}^2T_2)\dot{e}(t)\\ & - h_1\int_{t-h_1}^{t}\dot{e}^T(s)T_1\dot{e}(s)ds\\ & - h_{12}\int_{t-h_2}^{t-h_1}\dot{e}^T(s)T_2\dot{e}(s)ds. \end{aligned} \tag{42}$$

As in (18) and (19), condition (23) implies that there exist $\gamma_3 > 0$ and $\gamma_4 > 0$ such that

$$\begin{aligned} 0 &\le 2\gamma_3\{\vartheta_1e^T(t)e(t) - \Delta f^T(\bar{x}(t),x(t))e(t)\},\\ 0 &\le 2\gamma_4\{\vartheta_2e^T(t)e(t) + \vartheta_3\Delta f^T(\bar{x}(t),x(t))e(t)\\ &\quad - \Delta f^T(\bar{x}(t),x(t))\Delta f(\bar{x}(t),x(t))\}. \end{aligned} \tag{43}$$

Combining (43) with (42) and using Lemma 1, we obtain

$$\dot{V}_2(e(t)) \le \zeta_e^T\{\Omega_e + \Pi_2^T(h_1^2T_1+h_{12}^2T_2)\Pi_2\}\zeta_e, \tag{44}$$

where

$$\begin{aligned}\zeta_e^T &= [e^T(t)\ e^T(t-h_1)\ e^T(t-h(t))\ e^T(t-h_2)\ \varphi_3^T\ \varphi_4^T\\ &\quad \times \Delta f^T(\bar{x}(t),x(t))],\\ \varphi_3^T &= (\frac{1}{h_1}\int_{t-h_1}^{t}e(s)ds)^T,\quad \varphi_4^T = (\frac{1}{h_{12}}\int_{t-h_2}^{t-h_1}e(s)ds)^T. \end{aligned}$$

The time derivative of (34) along the trajectory of (21) is obtained as follows

$$\dot{V}(x(t),e(t)) = \dot{V}_1(x(t)) + \dot{V}_2(e(t)) \le \zeta^T\Omega\zeta, \tag{45}$$

where $\zeta^T = [\zeta_x^T\ \zeta_e^T]$. By considering the augmented system (21) with (22) and known K_i and L_i, Ω will be given by

$$\Omega = \sum_{i=1}^{2}\sum_{j=1}^{2}\theta_i(|\ \alpha_f(t)\ |)\theta_j(|\ \alpha_f(t)\ |)\Omega_{ij}. \tag{46}$$

Note that considering the conditions in (7) and (8), if Theorem 1 holds, then $\Omega < 0$, which implies that $\dot{V}(x(t), e(t)) < 0$. Thus, the closed-loop system (21) with known K_i and L_i is asymptotically stable, which completes the proof. □

APPENDIX B
PROOF OF THEOREM 2

By using the Schur complement, Ω can be rewritten as in (47), shown at the top of the next page, with

$$\begin{aligned}\beth(R_1^{-1*}) &= -P_{x11}R_1^{-1}P_{x11},\ \beth(R_2^{-1}) = -P_{x11}R_2^{-1}P_{x11},\\ \beth(T_1^{-1}) &= -P_{e11}T_1^{-1}P_{e11},\ \beth(T_2^{-1}) = -P_{e11}T_2^{-1}P_{e11}.\end{aligned}$$

Furthermore, Ω_{xe} and Γ_2^T can be rewritten as

$$\Omega_{xe} = \Sigma_1\underbrace{\begin{bmatrix}B_k\\ \mathbf{0}_{6n\times n}\end{bmatrix}}_{\mathbf{B}_k}\underbrace{\begin{bmatrix}-I_n & \mathbf{0}_{n\times 6n}\end{bmatrix}}_{\mathbf{I}},\quad \Gamma_2^T = \mathbf{I}^TB_k^T, \tag{48}$$

with $\Sigma_1 = diag\{P_{x11}, P_{x11}, P_{x11}, P_{x11}, P_{x11}, P_{x11}, I_n\}$.

To obtain the observer and controller gains, we define $X_{11} = P_{x11}^{-1}$ and $\Sigma = diag\{\Sigma_1^{-1}, \mathbf{I}_{7n}, I_n, I_n, P_{x11}^{-1}, P_{x11}^{-1}\}$. Then, pre and post multiplying Ω in (47) by Σ^T and its transpose respectively, we obtain

$$\tilde{\Omega} = \Sigma^T\Omega\Sigma = \tilde{\Omega}(0) + \mathrm{VL} + \mathrm{L}^T\mathrm{V}^T, \tag{49}$$

where, as shown in the equation at the top of the next page, with

$$\tilde{\Gamma}_1^T = \Sigma_1^{-1}\Gamma_1^T,\quad \tilde{\Omega}_x = \Sigma_1^{-1}\Omega_x\Sigma^{-1}.$$

$$\Omega = \begin{bmatrix} \Omega_x & \Omega_{xe} & 0_{7n\times n} & 0_{7n\times n} & h_1\Gamma_1^T P_{x11} & h_{12}\Gamma_1^T P_{x11} \\ * & \Omega_e & h_1\Pi_2^T P_{e11} & h_{12}\Pi_2^T P_{e11} & h_1\Gamma_2^T P_{x11} & h_{12}\Gamma_2^T P_{x11} \\ * & * & \beth(T_1^{-1}) & 0 & 0 & 0 \\ * & * & * & \beth(T_2^{-1}) & 0 & 0 \\ * & * & * & * & \beth(R_1^{-1}) & 0 \\ * & * & * & * & * & \beth(R_2^{-1}) \end{bmatrix}, \tag{47}$$

$$\tilde{\Omega}(0) = \begin{bmatrix} \tilde{\Omega}_x & 0_{7n} & 0_{7n\times n} & 0_{7n\times n} & h_1\tilde{\Gamma}_1^T & h_{12}\tilde{\Gamma}_1^T \\ * & \Omega_e & h_1\Pi_2^T P_{e11} & h_{12}\Pi_2^T P_{e11} & 0 & 0 \\ * & * & \beth(T_1^{-1}) & 0 & 0 & 0 \\ * & * & * & \beth(T_2^{-1}) & 0 & 0 \\ * & * & * & * & \beth(X_{11}R_1^{-1}X_{11}) & 0 \\ * & * & * & * & * & \beth(X_{11}R_2^{-1}X_{11}) \end{bmatrix},$$

$$\mathrm{V} = \begin{bmatrix} \mathbf{B}_k^T & \mathbf{0}_{n\times 9n} & h_1 B_k^T & h_2 B_k^T \end{bmatrix},$$

$$\mathrm{L} = \begin{bmatrix} \mathbf{0}_{n\times 7n} & \mathbf{I} & \mathbf{0}_{n\times 4n} \end{bmatrix}$$

Using Lemma 2, we obtain

$$\tilde{\Omega} \le \tilde{\Omega}(0) + \mathrm{V}(\epsilon X_{11})\mathrm{V}^T + \mathrm{L}^T(\epsilon X_{11})^{-1}\mathrm{L}. \tag{50}$$

Using the Schur complement Lemma, we have

$$\tilde{\Omega} \le \underbrace{\begin{bmatrix} \tilde{\Omega}(0) & \mathrm{V}X_{11} & \mathrm{L}^T \\ * & -\frac{1}{\epsilon}X_{11} & 0 \\ * & * & -\epsilon X_{11} \end{bmatrix}}_{\Xi}. \tag{51}$$

For a positive definite matrix, the following inequalities hold

$$\begin{aligned} &\beth(X_{11}R_1^{-1}X_{11}) \le \tilde{R}_1 - 2X_{11}, \quad \beth(T_1^{-1}) \le T_1 - 2P_{e11}, \\ &\beth(X_{11}R_2^{-1}X_{11}) \le \tilde{R}_2 - 2X_{11}, \quad \beth(T_2^{-1}) \le T_2 - 2P_{e11}. \end{aligned} \tag{52}$$

For a positive scalar ϵ, we have $-\frac{1}{\epsilon} \le -(2-\epsilon)$. By assuming $X_{11} > \delta_1 I$, we obtain

$$-\frac{1}{\epsilon}X_{11} \le -(2\delta_1 - \underbrace{\epsilon\delta_1}_{\delta_2})I, \quad -\epsilon X_{11} \le -\delta_2 I. \tag{53}$$

Define the following change of coordinates

$$\begin{aligned} \tilde{P}_{x22} &= X_{11}P_{x22}X_{11}, \quad \tilde{P}_{x33} = X_{11}P_{x33}X_{11}, \\ \tilde{R}_\ominus &= X_{11}R_\ominus X_{11}, \quad \ominus = \{1,2\}, \\ \tilde{Q}_\odot &= X_{11}Q_\odot X_{11}, \quad \odot = \{1,2,3\}. \end{aligned} \tag{54}$$

Substituting (53) and (52) from the right hand side of (51) and using (22) with the relaxation scheme in [36], we obtain

$$\begin{aligned} \Xi = &\sum_{i=1}^{2} \theta_i^2(|\ \alpha_f(t)\ |)\Xi_{ii} \\ &+ \sum_{i=1}^{2}\sum_{i<j}^{2} \theta_i(|\ \alpha_f(t)\ |)\theta_j(|\ \alpha_f(t)\ |)(\Xi_{ij} + \Xi_{ji}) \end{aligned} \tag{55}$$

Thus, one can see that if conditions (29) and (30) are satisfied, then (55) holds as well, implying that $\Omega < 0$, which completes the proof. □

REFERENCES

[1] J. Ma, Y. Ding, J. C. P. Cheng, Y. Tan, V. J. L. Gan, and J. Zhang, "Analyzing the leading causes of traffic fatalities using XGBoost and grid-based analysis: A city management perspective," *IEEE Access*, vol. 7, pp. 148059–148072, 2019.

[2] F. Wang and Y. Chen, "Dynamics and control of a novel active yaw stabilizer to enhance vehicle lateral motion stability," *J. Dyn. Syst., Meas., Control*, vol. 140, no. 8, pp. 7–81, Aug. 2018.

[3] W. Zhao, X. Qin, and C. Wang, "Yaw and lateral stability control for four-wheel steer-by-wire system," *IEEE/ASME Trans. Mechatronics*, vol. 23, no. 6, pp. 2628–2637, Dec. 2018.

[4] C. E. Beal and C. Boyd, "Coupled lateral-longitudinal vehicle dynamics and control design with three-dimensional state portraits," *Vehicle Syst. Dyn.*, vol. 57, no. 2, pp. 286–313, Feb. 2019.

[5] L. M. Ho, "Robust residual generator synthesis for uncertain LPV systems applied to lateral vehicle dynamics," *IEEE Trans. Control Syst. Technol.*, vol. 27, no. 3, pp. 1275–1283, May 2019.

[6] B. Gutjahr, L. Gröll, and M. Werling, "Lateral vehicle trajectory optimization using constrained linear time-varying MPC," *IEEE Trans. Intell. Transp. Syst.*, vol. 18, no. 6, pp. 1586–1595, Jun. 2017.

[7] J. Gallep, V. Govender, and S. Müller, "Model predictive lateral vehicle guidance using a position controlled EPS system," *IFAC-PapersOnLine*, vol. 50, no. 2, pp. 265–270, Dec. 2017.

[8] S. E. Li, H. Chen, R. Li, Z. Liu, Z. Wang, and Z. Xin, "Predictive lateral control to stabilise highly automated vehicles at tire-road friction limits," *Vehicle Syst. Dyn.*, vol. 58, no. 5, pp. 768–786, 2020.

[9] X.-H. Chang, Y. Liu, and M. Shen, "Resilient control design for lateral motion regulation of intelligent vehicle," *IEEE/ASME Trans. Mechatronics*, vol. 24, no. 6, pp. 2488–2497, Dec. 2019.

[10] H. Dahmani, O. Pagés, A. El Hajjaji, and N. Daraoui, "Observer-based robust control of vehicle dynamics for rollover mitigation in critical situations," *IEEE Trans. Intell. Transp. Syst.*, vol. 15, no. 3, pp. 274–284, Feb. 2014.

[11] M. Kchaou, "Robust H_∞ observer-based control for a class of (TS) fuzzy descriptor systems with time-varying delay," *Int. J. Fuzzy Syst.*, vol. 19, no. 3, pp. 909–924, Jun. 2017.

[12] H. Fan, M. Meng, and J.-E. Feng, "Observers of fuzzy descriptor systems with time-delays," in *Abstract and Applied Analysis*. London, U.K.: Hindawi, 2014.

[13] Y. Ma, J. Chen, X. Zhu, and Y. Xu, "Lateral stability integrated with energy efficiency control for electric vehicles," *Mech. Syst. Signal Process.*, vol. 127, pp. 1–15, Jul. 2019.
[14] W. Sun, X. Wang, and C. Zhang, "A model-free control strategy for vehicle lateral stability with adaptive dynamic programming," *IEEE Trans. Ind. Electron.*, vol. 67, no. 12, pp. 10693–10701, Dec. 2020.
[15] S. Cheng, L. Li, B. Yan, C. Liu, X. Wang, and J. Fang, "Simultaneous estimation of tire side-slip angle and lateral tire force for vehicle lateral stability control," *Mech. Syst. Signal Process.*, vol. 132, pp. 168–182, Oct. 2019.
[16] A. Seuret and F. Gouaisbaut, "Wirtinger-based integral inequality: Application to time-delay systems," *Automatica*, vol. 49, no. 9, pp. 2860–2866, Sep. 2013.
[17] H. El Aiss, A. Hmamed, and A. El Hajjaji, "Improved stability and H_∞ performance criteria for linear systems with interval time-varying delays via three terms approximation," *Int. J. Syst. Sci.*, vol. 48, no. 16, pp. 3450–3458, Dec. 2017.
[18] Y. Xia, M. Fu, and P. Shi, *Analysis and Synthesis of Dynamical Systems With Time-Delays*, vol. 387. Cham, Switzerland: Springer, 2009.
[19] M. Kchaou, M. Souissi, and A. Toumi, "Robust reliable guaranteed cost piecewise fuzzy control for discrete-time nonlinear systems with time-varying delay and actuator failures," *Int. J. Gen. Syst.*, vol. 40, no. 5, pp. 531–558, Jul. 2011.
[20] H. Gassara, A. E. Hajjaji, M. Kchaou, and M. Chaabane, "Robust H_∞ reliable control of time delay nonlinear systems via Takagi–Sugeno fuzzy models," *Int. J. Syst. Sci.*, vol. 45, no. 3, pp. 667–681, 2014.
[21] V. Cerone, D. Piga, and D. Regruto, "Set-membership LPV model identification of vehicle lateral dynamics," *Automatica*, vol. 47, no. 8, pp. 1794–1799, Aug. 2011.
[22] M. Mitschke, "Das einspurmodell von Riekert–Schunck," *ATZ Automobiltechnische Zeitschrift*, vol. 107, no. 11, pp. 1030–1031, Nov. 2005.
[23] C. Latrach, M. Kchaou, and H. Guéguen, "H_∞ observer-based decentralised fuzzy control design for nonlinear interconnected systems: An application to vehicle dynamics," *Int. J. Syst. Sci.*, vol. 48, no. 7, pp. 1485–1495, May 2017.
[24] C. Latrech, M. Kchaou, and H. Guéguen, "Networked non-fragile H_∞ static output feedback control design for vehicle dynamics stability: A descriptor approach," *Eur. J. Control*, vol. 40, pp. 13–26, Mar. 2018.
[25] M. Ersoy and B. Heißing, *Chassis Handbook: Fundamentals, Driving Dynamics, Components, Mechatronics, Perspectives*. Cham, Switzerland: Springer, 2011.
[26] D. Schramm, M. Hiller, and R. Bardini, *Vehicle Dynamics: Modeling and Simulation*. Cham, Switzerland: Springer, 2014.
[27] S. Wei, Y. Zou, X. Zhang, T. Zhang, and X. Li, "An integrated longitudinal and lateral vehicle following control system with radar and vehicle-to-vehicle communication," *IEEE Trans. Veh. Technol.*, vol. 68, no. 2, pp. 1116–1127, Feb. 2019.
[28] D. Piyabongkarn, R. Rajamani, J. A. Grogg, and J. Y. Lew, "Development and experimental evaluation of a slip angle estimator for vehicle stability control," *IEEE Trans. Control Syst. Technol.*, vol. 17, no. 1, pp. 78–88, May 2008.
[29] Z. Wang, M. Dong, Y. Qin, Z. Wang, T. Xu, X. Shi, and L. Gu, "Fuzzy observer for nonlinear vehicle system roll behavior with coupled lateral and vertical dynamics," SAE Tech. Paper 2018-01-0559 2018.
[30] H. Dahmani, M. Chadli, A. Rabhi, and A. EI Hajjaji, "Vehicle dynamic estimation with road bank angle consideration for rollover detection: Theoretical and experimental studies," *Vehicle Syst. Dyn.*, vol. 51, no. 12, pp. 1853–1871, Sep. 2013.
[31] K. Gu, J. Chen, and V. L. Kharitonov, *Stability of Time-Delay Systems*. Cham, Switzerland: Springer, 2003.
[32] G. Wanner and E. Hairer, *Solving Ordinary Differential Equations II*, vol. 375. Berlin, Germany: Springer, 1996.
[33] K. Zhou and P. P. Khargonekar, "Robust stabilization of linear systems with norm-bounded time-varying uncertainty," *Syst. Control Lett.*, vol. 10, no. 1, pp. 17–20, Jan. 1988.
[34] S. Boyd, L. El Ghaoui, E. Feron, and V. Balakrishnan, *Linear Matrix Inequalities in System and Control Theory*. Philadelphia, PA, USA: SIAM, 1994.
[35] N. El Youssfi, R. El Bachtiri, T. Zoulagh, and H. El Aiss, "Unknown input observer design for vehicle lateral dynamics described by Takagi–Sugeno fuzzy systems," *Optim. Control Appl. Methods*, vol. 43, no. 2, pp. 354–368, Mar. 2022.
[36] X.-H. Chang, *Takagi–Sugeno Fuzzy Systems Non-Fragile H-Infinity Filtering*, vol. 282, Cham, Switzerland: Springer, 2012.

HICHAM EL AISS (Member, IEEE) received the master's degree in signals systems and informatics and the Ph.D. degree in electrical engineering from the Faculty of Sciences, University of Sidi Mohamed Ben Abdellah, in 2013 and 2018, respectively. From 15 March 2019 to 15 March 2022, he was a Postdoctoral Researcher at the University of Santiago, Chile, under grant N:3190378. He is currently working with the Chile's University of Santiago. His current research interests include delay systems, stability theory, robust control, fuzzy control, vehicle dynamics, and descriptor systems.

KARINA A. BARBOSA (Senior Member, IEEE) received the B.S. degree in applied mathematical from the Universidade Federal do Rio Grande do Sul, Porto Alegre, Brazil, in 1997, and the master's and doctor degrees in electrical engineering from the Universidade Federal de Santa Catarina, Florianópolis, Brazil, in 1999 and 2003, respectively. From 2005 to 2007, she held a postdoctoral position at Laboratório Nacional de Computacão Científica (LNCC/MCT), Petrópolis, Brazil. She was an Academic Visitor at the Centre for Complex Dynamic Systems and Control (CDSC), The University of Newcastle, Australia, from August 2007 to June 2008. In 2009, she was a Postdoctoral Fellow at the Department of Electrical Engineering of Pontificia Universidad Católica de Chile, Santiago, Chile. Currently, she is a full-time Associate Professor with the Department of Electrical Engineering, Universidad de Santiago de Chile. Since 2011, she has been a part of the Chilean Automatic Control Society (ACCA) Board of Directors. Her research interests include robust and LPV filtering, control design, descriptor systems, and robust control applications.

ANDRÉS A. PETERS (Member, IEEE) was born in Coyhaique, Chile, in 1983. He received the B.S. and M.S. degrees in electronic engineering from the Technical University Federico Santa María (UTFSM), Valparaíso, Chile, in 2007, and the Ph.D. degree in mathematics from the Hamilton Institute at Maynooth University, Maynooth, Co. Kildare, Ireland, in 2015. From 2015 to 2019, he was a Principal Investigator for a postdoctoral research grant at the Electronic Engineering Department of UTFSM. He was an Assistant Professor at the Department of Electrical Engineering, Universidad Tecnológica Metropolitana, from 2019 to 2021. Since 2021, he has been an Assistant Professor with the Faculty of Engineering and Sciences of the Universidad Adolfo Ibáñez, Santiago, Chile. His research interests include the applications of control theory in multi-agent and networked systems and the study of performance bounds for optimal control of linear systems.